Received: 21 December 2023 | Revised: 10 April 2024 | Accepted: 11 May 2024

DOI: 10.1002/ajmg.c.32089

RESEARCH ARTICLE

AMERICAN JOURNAL OF medical genetics PART C Seminars in Medical Genetics

WILEY

# Blepharophimosis with intellectual disability and Helsmoortel-Van Der Aa Syndrome share episignature and phenotype

Camilla Sarli[1] | Liselot van der Laan[2] | Jack Reilly[3] | Slavica Trajkova[4,5] | Diana Carli[4] | Alfredo Brusco[4,6,7] | Michael A. Levy[8] | Raissa Relator[8] | Jennifer Kerkhof[8] | Haley McConkey[3,8] | Matthew L. Tedder[9] | Cindy Skinner[9] | Mariëlle Alders[2] | Peter Henneman[2] | Raoul C. M. Hennekam[2] | Claudia Ciaccio[10] | Stefano D'Arrigo[10] | Antonio Vitobello[11] | Laurence Faivre[12,13] | Sacha Weber[14,15] | Aline Vincent-Devulder[11] | Laurence Perrin[11] | Alexia Bourgois[11] | Toshiyuki Yamamoto[16] | Kay Metcalfe[17,18] | Marcella Zollino[19,20] | Usha Kini[21] | Daniela Oliveira[22] | Sergio B. Sousa[22] | Denise Williams[23] | Gerarda Cappuccio[1] | Bekim Sadikovic[2,3,8] | Nicola Brunetti-Pierri[1,24,25]

[1]Department of Translational Medicine, Federico II University of Naples, Naples, Italy

[2]Department of Human Genetics, Amsterdam Reproduction & Development Research Institute, Amsterdam University Medical Centers, University of Amsterdam, Amsterdam, The Netherlands

[3]Department of Pathology and Laboratory Medicine, Western University, London, Ontario, Canada

[4]Department of Medical Sciences, University of Torino, Turin, Italy

[5]Molecular Biotechnology Center "Guido Tarone", University of Turin, Turin, Italy

[6]Medical Genetics Unit, Città della Salute e della Scienza University Hospital, Turin, Italy

[7]Department of Neurosciences Rita Levi-Montalcini, University of Turin, Turin, Italy

[8]Verspeeten Clinical Genome Centre, London Health Science Centre, London, Ontario, Canada

[9]Greenwood Genetic Center, Greenwood, South Carolina, USA

[10]Department of Pediatric Neurosciences, Fondazione IRCCS Istituto Neurologico Carlo Besta, Milan, Italy

[11]Department of Genetics, UNICAEN, Caen University Hospital, Normandy University, Caen, France

[12]Université de Bourgogne, Inserm U1231, Equipe GAD, Dijon, France

[13]CHU Dijon Bourgogne, Centre de Génétique, Centre de Référence Maladies Rares "Anomalies du Développement et Syndromes Malformatifs", FHU-TRANSLDAD, Dijon, France

[14]Service de Génétique, CHU de Caen-Normandie, Caen, France

[15]Service de Neurologie, CHU de Caen-Normandie, Caen, France

[16]Division of Gene Medicine, Graduate School of Medical Science, Tokyo Women's Medical University, Tokyo, Japan

[17]Manchester Centre for Genomic Medicine, St Mary's Hospital, Health Innovation Manchester, Manchester University Foundation NHS Trust, Manchester, UK

[18]Division of Evolution, Infection and Genomics, School of Biological Sciences, Faculty of Biology, Medicine and Health, The University of Manchester, Manchester, UK

Camilla Sarli, Liselot van der Laan, and Jack Reilly jointly coordinated to this study.

Bekim Sadikovic and Nicola Brunetti-Pierri jointly coordinated to this study.

[19]Institute of Genomic Medicine, Department of Life Sciences and Public Health, 'Sacro Cuore' Catholic University of Rome, Rome, Italy

[20]Medical Genetics Unit, Foundation IRCCS AOU Policlinico 'A. Gemelli', Rome, Italy

[21]Oxford Centre for Genomic Medicine, Oxford University Hospitals NHS Foundation Trust, Oxford, UK

[22]Medical Genetics Unit, Hospital Pediátrico, Centro Hospitalar e Universitário de Coimbra, Coimbra, Portugal

[23]Department of Clinical Genetics, Birmingham Women's & Children's NHS Foundation Trust, Birmingham, UK

[24]Telethon Institute of Genetics and Medicine, Pozzuoli, Italy

[25]Scuola Superiore Meridionale (SSM, School of Advanced Studies), Genomics and Experimental Medicine Program, University of Naples Federico II, Naples, Italy

**Correspondence**
Bekim Sadikovic, Verspeeten Clinical Genome Centre, London Health Science Centre, London, Ontario, Canada
Email: bekim.sadikovic@lhsc.on.ca

Nicola Brunetti-Pierri, Department of Translational Medicine, Federico II University of Naples, Naples, Italy.
Email: brunetti@tigem.it

**Present address**
Gerarda Cappuccio, Department of Pediatrics—Neurology, Baylor College of Medicine, Houston, Texas, USA.

**Funding information**
Telethon Foundation, Telethon Undiagnosed Diseases Program; Genome Canada and the Ontario Genomics Institute

## Abstract

Blepharophimosis with intellectual disability (BIS) is a recently recognized disorder distinct from Nicolaides-Baraister syndrome that presents with distinct facial features of blepharophimosis, developmental delay, and intellectual disability. BIS is caused by pathogenic variants in *SMARCA2*, that encodes the catalytic subunit of the superfamily II helicase group of the BRG1 and BRM-associated factors (BAF) forming the BAF complex, a chromatin remodeling complex involved in transcriptional regulation. Individuals bearing variants within the bipartite nuclear localization (BNL) signal domain of *ADNP* present with the neurodevelopmental disorder known as Helsmoortel-Van Der Aa Syndrome (HVDAS). Distinct DNA methylation profiles referred to as episignatures have been reported in HVDAS and BAF complex disorders. Due to molecular interactions between *ADNP* and BAF complex, and an overlapping craniofacial phenotype with narrowing of the palpebral fissures in a subset of patients with HVDAS and BIS, we hypothesized the possibility of a common phenotype-specific episignature. A distinct episignature was shared by 15 individuals with BIS-causing *SMARCA2* pathogenic variants and 12 individuals with class II HVDAS caused by truncating pathogenic *ADNP* variants. This represents first evidence of a sensitive phenotype-specific episignature biomarker shared across distinct genetic conditions that also exhibit unique gene-specific episignatures.

**KEYWORDS**
ADNP, blepharophimosis with intellectual disability, Helsmoortel-Van Der Aa Syndrome, SMARCA2

## 1 | INTRODUCTION

Blepharophimosis with intellectual disability (BIS, OMIM# 619293) is a recently described disorder distinct from Nicolaides-Baraister syndrome (NCBRS) caused by pathogenic variants in *SMARCA2* (Cappuccio et al., 2020). *SMARCA2* encodes the catalytic subunit of the superfamily II helicase group of the BRG1 and BRM-associated factors (BAF) forming the BAF complex, a chromatin remodeling complex that regulates expression of several genes. BIS-causing variants were found to cluster around an alpha-helix domain, that defines an interaction surface with other subunits of the BAF complex. Distinct genome wide DNA methylation biomarkers detectable in patient's peripheral blood, referred to as episignatures, can also differentiate NCBRS from BIS (Cappuccio et al., 2020).

Helsmoortel-Van Der Aa Syndrome (HVDAS, OMIM #615873) is a neurodevelopmental disorder caused by pathogenic variants in the *ADNP* gene presenting with developmental delay, intellectual disability, autism spectrum disorder, and facial dysmoprhisms (Breen et al., 2020). *ADNP* encodes a protein interacting with the chromatin remodeling complex, thus controlling chromatin structure and accessibility by chromatin remodelers. Similar to patients harboring *SMARCA2* pathogenic variants (NCBRS or BIS), *ADNP* pathogenic variants have been shown to be associated with two distinct episignatures associated with pathogenic variants in either the terminal or central protein domain (Bend et al., 2019). The two episignatures, denoted as class I (characterized by predominantly hypomethylation) and class II (exhibiting predominant hypermethylation), have also been associated with minor phenotypic differences (Breen et al., 2020) with a molecular mechanism still awaiting clarification. *ADNP* negatively regulates its expression by binding its own promoter, hence, truncating variants causing reduction in protein level may result in loss of the

negative feedback autoregulation of ADNP expression (Oz et al., 2012). In contrast, partial loss of function variants may retain the ADNP negative feedback loop, thus resulting in different episignature profiles (Vandeweyer et al., 2014). It has also been hypothesized that the mutant ADNP competes with the wild-type protein for binding to the BAF complex, the orthologue of the yeast SWI/SNF complex. *ADNP* was found to bind directly to *SMARCA2*, *SMARCA4*, and *SMARCC2* through its C-terminal end (Helsmoortel et al., 2014).

A recognizable pattern of dysmorphic features in HVDAS includes prominent forehead, high anterior hairline with sparse hair, down-slanted palpebral fissures, prominent eyelashes, wide and depressed nasal bridge, and short nose with full nasal tip. In contrast to BIS, dysmorphology differences among the two groups of HVDAS patients with distinct episignatures have not yet been reported. Among patients harboring *ADNP* pathogenic variants, we noted a subset of patients harboring variants of class II of methylation within or near the bipartite nuclear localization (BNL) domain show narrow palpebral fissures as well as overt blepharophimosis overlapping the BIS phenotype. In the present study, we investigated the hypothesis of a common, sensitive, and specific whole-genome episignature in patients with the overlapping phenotypes of BIS and HVDAS with class II variants in *ADNP* gene.

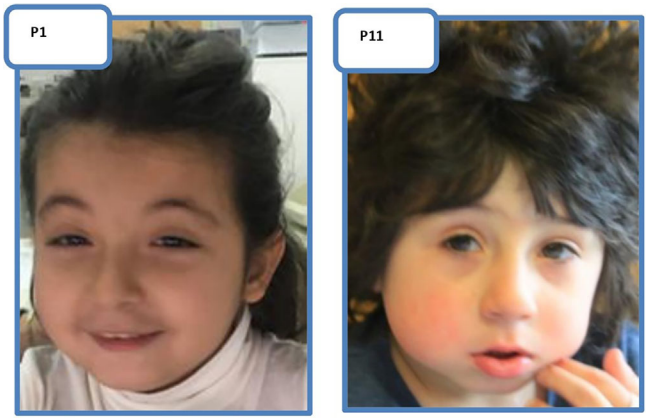


**FIGURE 1** Facial appearance of two new patients (P1 and P11) from our cohort carrying ADNP-class II of methylation variants (Patients P2, P3, P4, P6, and P7 of our cohort are illustrated in Bend et al., 2019). Note the atypical presentation with no sparse hair or down-slanting palpebral fissures, but instead with narrow and short palpebral fissures or blepharophimosis.

## 2 | MATERIALS AND METHODS

### 2.1 | Editorial policies and ethical considerations

The study was conducted in accordance with the regulations of the Western University research Ethics board (REB116108 and REB106302). We obtained written informed consent from the participants or their substitute decision maker to publish patients' clinical and genetic information. Explicit consent for the publication of individual's photographs is obtained separately for individuals shown in Figure 1.

### 2.2 | Study cohort

For this study, we included a total of 31 individuals (16 females and 15 males) with variants in *ADNP* (HVDAS) and *SMARCA2* (BIS). We divided this cohort in the discovery cohort ($n = 23$) that was used for the probe selection purpose and construction of the classification model for the BIS-HVDAS episignature. The other 8 individuals were used for validation ($n = 4$) and to assess the non-NCBRS-non-BIS ($n = 4$). Variants were classified according to the guidelines of the American College of Medical Genetics (ACMG) and Association for Molecular Pathology (AMP) (Richards et al., 2015; Riggs et al., 2020).

### 2.3 | DNA methylation

We performed DNA isolation and bisulfite on 31 individuals according to standard techniques. EPIC array (San Diego, CA) was performed on bisulfited converted genomic DNA based on manufactures protocol. The intensity data files (idats) were generated and loaded into R (version 4.2.3) (Aryee et al., 2014) with minfi (version 1.44.0). The used quality control and feature selection methods were published in detail before (Aref-Eshghi et al., 2019; Levy, McConkey, et al., 2022). Briefly, normalization, background correction and evaluation of the density plots were performed, and quality control checks for age and sex were conducted. Before analyses the following probes were removed; probes that overlap with single-nucleotide variation, probes that are cross-reactive, probes specific to regions on the X or Y chromosomes and probes with detection $p$-value >0.1. After removal, 772,557 were remained.

### 2.4 | DNA methylation analyses

DNA methylation analyses were performed based on previously published methods (Aref-Eshghi et al., 2019; Levy, McConkey, et al., 2022). To summarize, matched controls from the EpiSign™ knowledge Database (EKD) were selected based on batch type, array type, sex and age with MatchIt (version 4.5.2) (Ho et al., 2011). Principal component analyses (PCA) were used for feature selection, and to detect possible outliers in our training and matched control cohorts. We performed differentially methylation analyses with limma (version 3.54.2) (Ritchie et al., 2015) with linear regression fitting. For this analysis, we used methylation beta values as predictors and analyses methylation labels as response, adjusting the model for estimate blood cell counts as confounding variables. We applied the empirical Bayes method adjusted by the Benjamini-Hochberg procedure to control for false discoveries with $t$-statistics and $p$-values. We experimented with various cutoffs for the top $p$-values and measurements of variable importance across different probe sets to identify the most optimized results. Finally, we investigated the separate clustering between our

**TABLE 1** Genotype and American College of Medical Genetics (ACMG) classification in cases of our cohort.

| Case | Sex | Label | Genotype | ACMG° |
|---|---|---|---|---|
| 1 | F | ADNP-BNL | c.2157C>A, p.(Tyr719*) | PVS1, PS2, PM2 |
| 2 | F | ADNP-BNL | c.2157C>A, p.(Tyr719*) | PVS1, PS2, PM2 |
| 3 | F | ADNP-BNL | c.2157C>A, p.(Tyr719*) | PVS1, PS2, PM2 |
| 4 | F | ADNP-BNL | c.2157C>A, p.(Tyr719*) | PVS1, PS2, PM2 |
| 5 | M | ADNP-BNL | c.2156dup, p.(Tyr719*) | PVS1, PS2, PM2 |
| 6 | M | ADNP-BNL | c.2188C>T, p.(Arg730*) | PVS1, PS2, PM2 |
| 7 | M | ADNP-BNL | c.2287del, p.(Ser763Profs*9) | PVS1, PS2, PM2 |
| 8 | M | ADNP-BNL | c.2157C>A, p.(Tyr719*) | PVS1, PS2, PM2 |
| 9 | F | ADNP-BNL | c.2156dup, p.(Tyr719*) | PVS1, PS2, PM2 |
| 10 | F | ADNP-BNL | c.2157C>G, p.(Tyr719*) | PVS1, PS2, PM2 |
| 11 | F | ADNP-BNL_validation | c.2157del, p.(Tyr719*) | PVS1, PS2, PM2 |
| 12 | F | ADNP-BNL_validation | c.2156dup, p.(Tyr719*) | PVS1, PS2, PM2 |
| 13 | M | BIS | c.1585C>G, p.(Leu529Val) | PS2, PM1, PP2, PP3, PM2 |
| 14 | M | BIS | c.2810G>A, p.(Arg937His) | PS2, PM1, PP2, PP3, PM2, PM5 |
| 15 | M | BIS | c.2810G>A, p.(Arg937His) | PS2, PM1, PP2, PP3, PM2, PM5 |
| 16 | M | BIS | c.2810G>A, p.(Arg937His) | PS2, PM1, PP2, PP3, PM2, PM5 |
| 17 | M | BIS | c.2809C>T, p.(Arg937Cys) | PS2, PM1, PP2, PP3, PM2, PM5 |
| 18 | M | BIS | c.2809C>T, p.(Arg937Cys) | PS2, PM1, PP2, PP3, PM2, PM5 |
| 19 | M | BIS | c.1538G>T, p.(Gly513Val) | PS2, PS3, PM1, PP2, PM2, PM5 |
| 20 | F | BIS | c.2809C>T, p.(Arg937Cys) | PS2, PM1, PP2, PP3, PM2, PM5 |
| 21 | F | BIS | c.1573C>T, p.(Arg525Cys) | PS2, PS3, PM1, PP2, PM2, PM5 |
| 22 | F | BIS | c.2566A>G, p.(Met856Val)* | PS2, PS3, PM1, PP2, PM2, PM5 |
| 23 | M | BIS | c.1573C>T, p.(Arg525Cys) | PS2, PS3, PM1, PP2, PM2, PM5 |
| 24 | F | BIS | c.1574G>A, p.(Arg525His) | PS2, PS3, PM1, PP2, PM2, PM5 |
| 25 | F | BIS | c.1534G>A, p.(Glu512Lys) | PS2, PS3, PM1, PP2, PM2, PM5 |
| 26 | F | BIS_validation | c.1585C>G, p.(Leu529Val) | PS2, PS3, PM1, PP2, PM2, PM5 |
| 27 | F | BIS_validation | c.6286C>A, p.(Asp510Gly) | NA |
| 28 | M | BIS_atypical | c.2296C>G, p.(Leu766Val) | NA |
| 29 | M | BIS_atypical | c.2296C>G, p.(Leu766Val) | NA |
| 30 | M | BIS_atypical | c.2296C>G, p.(Leu766Val) | NA |
| 31 | M | BIS_atypical | c.1458C>G, p.(Asn486Lys) | NA |

*Note:* F, female; M, male; NM_003070.3 (SMARCA2) and NM_001282532.3 (ADNP) ACMG° criteria applied (Richards et al., 2015).

cases and controls with heatmaps and multidimensional scaling (MDS) with ggplots2 (version 3.1.3), afterwards the best clustering method was selected. To test the reproducibility of the discovered episignature, we performed leave one-out cross validation.

## 2.5 | Prediction model

To test whether our signature was sensitive and specific, support vector machine (SVM) was used. We trained with e1071 (version 1.7-13) using the selected features and our matched controls and cases as training. The classifier was constructed by using the training samples against the matched control samples that were used for probe selection, 75% of other controls and samples with known episignatures from the EKD and the remaining 25% of these controls and samples with known episignatures were used for model testing. The classifier generated a score methylation variant pathogenicity (MVP score) ranging from 0 to 1 for each sample, that indicates change that the sample has a methylation profile similar of that of our cohorts.

## 2.6 | Overlap of the BIS-HVDAS genome-wide DNA methylation profile with other neurodevelopmental disorders on EpiSign™

We performed functional annotation analyses to compare our BIS-HVDAS episignature with the other 56 EpiSign™ disorders based on previously published articles (Levy, Relator, et al., 2022; Rooney

**TABLE 2** Summary of clinical features of our patients with ADNP pathogenic variants clustering within the bipartite nuclear localization signal, highlighting in the square the atypical ocular features.

| | BIS[a] | HVDAS[b] | ADNP-BNL | Characteristic cranio-facial features | BIS[a] | HVDAS[b] | ADNP-BNL |
|---|---|---|---|---|---|---|---|
| Growth parameters | | | | Coarse face | | 17% | - |
| Low birth weight | 36% | - | - | Prominent forehead | ~50% | 65% | 28% (2/7) |
| Short birth length | 29% | - | - | Low/High anteriore hairline | ~50% | 50% | 42% (3/7) |
| Short stature (≤2 SD) | 25% | 23% | 42% (3/7) | Broad nasal bridge | 71% | 50% | 28% (2/7) |
| Microcephaly | 43% | - | 14% (1/7) | Upturned nasal tip | 21% | 47% | 28% (2/7) |
| Macrocephaly | - | - | 28% (2/7) | Short nose | 28% | 49% | 28% (2/7) |
| Neurodevelopmental features | | | | Long philtrum | 42% | 40% | 42% (3/7) |
| DD/ID | 100% | 100% | 71% (5/7) | Thin upper vermillion | 86% | 70% | 71% (5/7) |
| Hypotonia<br>Dealyed walking | 75%<br>70% | 78%<br>86.8% | 57% (4/7) | Everted lower vermillion | - | 70% | 42% (3/7) |
| Speech delay<br>Absent Speech | 70%<br>35% | 98.6%<br>90% | 100% (7/7) | Abnormal ears | 64% | ~50% | - |
| Behavioral problems<br>• Autism | 65% | 93%<br>~67% | 85.7% (6/7) | Ocular features | | | |
| Seizures | 21% | 16% | - | Vision issue | 64% | 74% | 14% (1/7) |
| Sleep disturbance<br>Sleep apnea | - | 65.2%<br>32% | 85.7% (6/7)<br>28% (2/7) | Ptosis | 14% | Some | 28% (2/7) |
| Other findings | | | | Strabismus | 14% | ~50% | 14% (1/7) |
| Brain abnormalities | ~40% | 56% | 71% (5/7) | Myopia/hypermetropia | 42% | 5%–40% | 14% (1/7) |
| Hearing loss | 0% | 32% | - | Downslanting palpebral fissures | | 33% | - |
| Limb anomalies | 0%–30% | 62% | - | Narrow palpebral fissures | 71% | - | 85.7% (6/7) |
| Musculoskeletral features | 0%–25% | 55% | - | Blefarophimosis | 100% | - | 42% (3/7) |
| Gastrointestinal/feeding issues | 46% | 83% | 57% (4/7) | Epicanthus | 100% | - | 42% (3/7) |
| | | | | Hypertelorism | 57% | Some | - |

*Note:* Details on each subject of our cohort are provided in Table S4.
Abbreviations: BIS, Blepharophimosis with intellectual disability; DD; developmental delay; HVDAS, Helsmoortel-Van Der Aa Syndrome; ID; Intellectual disability.
[a]From Cappuccio et al. (2020) and [b] Van Dijck et al. (2019).

et al., 2023; van der Laan et al., 2022). Briefly, the percentage of DMPs shared between our BIS-HVDAS episignature and 56 genetic episignature disorders included in the EpiSign™ v3 clinical classifier were assessed. With pheatmap (version 1.0.12) we generated the heatmap and with circlize (version 0.4.15) (Gu et al., 2014) the circos plot. Clustering analyses were performed to detect relationships between all the cohorts with known episignatures and we produced this into a tree and leaf plot to show the distance and similarities with TreeAndLeaf (version 1.6.1) (Cardoso et al., 2022). Finally, we annotated all probes in relation to CpG island (CGIs) and genes with annotatr (version 1.20.0) (Cavalcante & Sartor, 2017) with AnnotationHub (version 3.2.2) to discover the genomic location of the selected DMPs as described previously by Levy, Relator, et al. (2022).

## 3 | RESULTS

Twelve unrelated individuals (including 8 female and 4 male subjects with an age range from 3 to 13 years) carrying de novo nonsense pathogenic *ADNP* class II variants and 15 individuals (from 14 families, including 8 female subjects and 7 male subjects with an age range from 1 to 17.5 years) with de novo *SMARCA2* pathogenic variants resulting in BIS, were analyzed to compare their episignature and phenotype profiles. All 12 subjects carrying a pathogenic variant in the *ADNP* genes belong to the class II of methylation subgroup, and 8 of these cases have been previously reported (Bend et al., 2019). Among the *ADNP* variants, 11 were nonsense within the BNL-domain and one a frameshift-stop variant outside the BNL-domain. Among nonsense variants, 10 individuals harbored the p.(Tyr719*) variant, while the other two harbored either the p.(Arg730*) variant or the p.(Ser763Profs*) variant. All *ADNP* variants were de novo and absent in the general population database (ACMG criteria PS2, PM2) (Table 1).

The 15 individuals with de novo missense *SMARCA2* variants all had the BIS phenotype and 10 of them were previously described (Cappuccio et al., 2020). Patients bearing *ADNP* pathogenic variants usually presented with hypotonia, severe language and motor delay,

**TABLE 3** Clinical and molecular features of patients with ADNP BNL domain variants.

| Clinical features | Pascolini et al. (2018) Patient 1 | Pascolini et al. (2018) Patient 2 | Helsmoortel et al. (2014) Patient 4 | Helsmoortel et al. (2014) Patient 5 | Helsmoortel et al. (2014) Patient 10 | Krajewska-Walasek et al. (2016) | Takenouchi et al. (2017) |
|---|---|---|---|---|---|---|---|
| Developmental delay | + | + | + | + | + | + | + |
| Autism | + | NK | + | + | + | NK | NK |
| Hypotonia | + | + | + | + | − | | NK |
| Seizures | − | − | − | − | − | − | − |
| Cerebral malformation | NK | + | + | + | − | − | − |
| Microcepaly | − | − | − | − | NK | − | + |
| Facial anomalies | + | + | + | + | NK | + | + |
| Blepharophimosis | + | + | + | + | + | + | + |
| Epicanthal folds | + | − | − | − | NK | + | + |
| Ptosis | + | + | + | + | NK | + | + |
| Hypertelorism | + | − | − | − | NK | + | − |
| Broad nasal bridge | + | − | + | − | NK | + | + |
| Dental anomalies | − | + | − | − | NK | NK | NK |
| Cleft palat | − | − | − | − | NK | + | − |
| Overweight | + | − | − | + | NK | − | − |
| Feeding difficulties | − | + | + | − | + | NK | − |
| Cardiac defect | − | + | − | NK | − | + | − |
| Hand anomalies | + | + | + | − | NK | + | + |
| Genitourinary anomalies | + | − | − | NK | NK | + | − |
| Gene | *ADNP* | *ADNP* | *ADNP* | *ADNP* | *ADNP* | *ADNP* | *ADNP* |
| Variant | c.2157C>G; p.Tyr719* | c.2188C>T; p.Arg730* | c.2153_2165del CTTACGAGCAAAT; p.Thr718Glyfs*12 | c.2157C>G; p.Tyr719* | c.2156_2157insA; p.Tyr719* | c.2188C>T; p.Arg730* | c.2157C > G; p.Tyr719* |

Abbreviation: NK, Not known; NM_001282532.3 (ADNP).

mild to severe intellectual disability, and characteristic facial features like prominent forehead, high frontal hairline, down slanting palpebral fissures, broad and depressed nasal bridge, and short nose with full, upturned tip (based on a cohort of 78 individuals) (Van Dijck et al., 2019). Detailed clinical information available in 7 of 12 HVDAS patients showed intellectual disability with severe speech delay and behavioral problems with autism spectrum disorders. About 57% (4/7) of patients had hypotonia and 85% (6/7) sleep disturbances, but epilepsy was rare. Several patients showed atypical shape of the eyelids that were noted to be narrow with blepharophimosis (Figure 1) in almost 85% *ADNP* subset (6 of 7) (Table 2). A review of the published cases with available facial pictures reveled other 7 HVDAS patients with blepharophimosis (Table 3). Although vision problems (e.g., strabismus and cortical visual impairment) have been reported in almost 75% of patients with HVDAS (Van Dijck et al., 2019), they were less common, only 14% (1 of 7), in our cohort.

### 3.1 | Identification and validation of the BIS-HVDAS episignature

We detected that individuals with pathogenic variants in *ADNP* and *SMARCA2* have a detectable DNA methylation change compared to unaffected controls. Two hundred and twelve differentially methylated CpG probes were selected (Table S1) and showed a significant separation between our BIS-HVDAS discovery cases (cases 1–10 and 13–25) and unaffected controls in unsupervised clustering methods, specifically hierarchical clustering (heatmap) and multidimensional scaling (MDS) (Figure S1). We tested the reproducibility of our BIS-HVDAS episignature with leave-25%-out cross validation, using the unsupervised and hierarchical clustering methods and MVP scores. During cross validation, all BIS-HVDAS cases correctly clustered together with the testing cases (Figure S2).

Validation of the BIS-HVDAS episignature was performed on four additional samples with variants in *ADNP* and *SMARCA2* labeled as

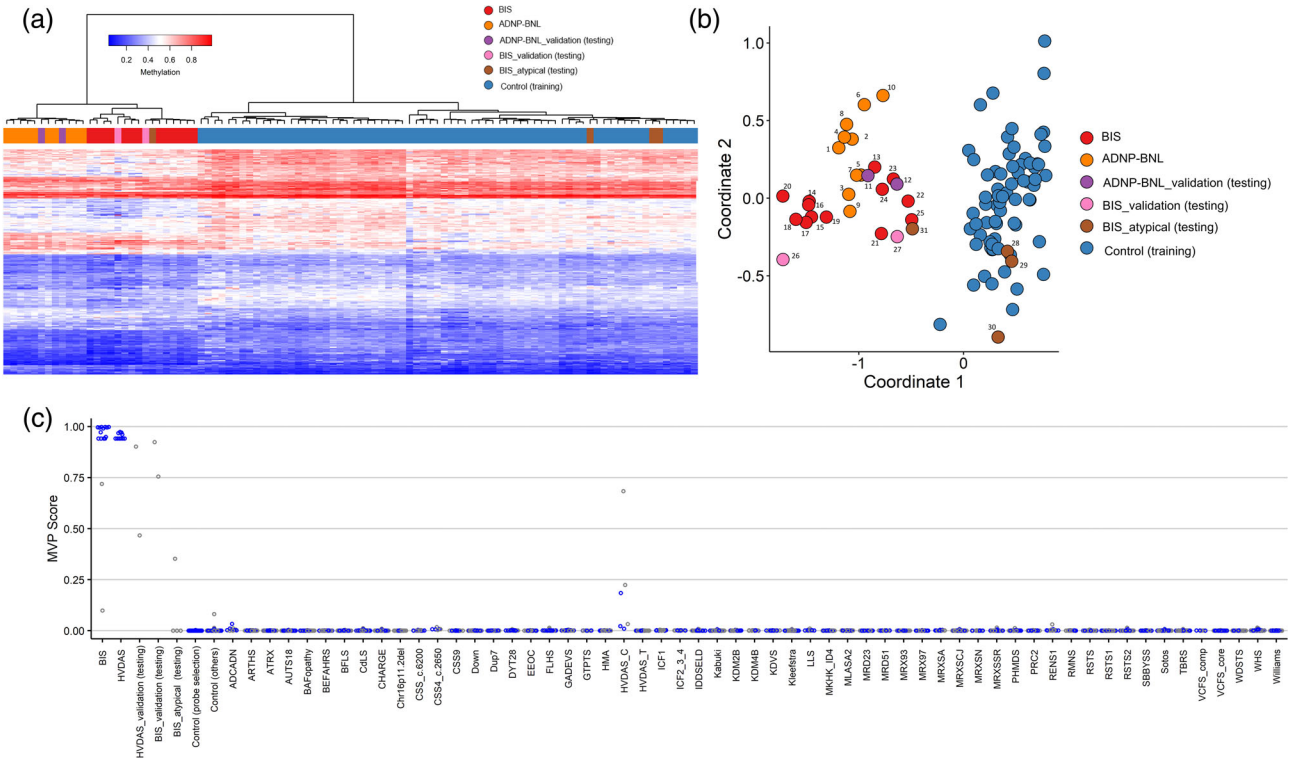


**FIGURE 2** Assessment of the Blepharophimosis-impaired intellectual development syndrome and Helsmoortel-van der Aa syndrome (BIS-HVDAS) episignature. **(a)** Euclidean hierarchical clustering heatmap, each column represents one BIS-HVDAS case or control, each row represents one probe selected for this episignature. This heatmap shows clear separation between BIS-HVDAS cases (red, orange, purple, and pink) used for training and validation from controls (blue). All the non-NCBRS-non-BIS (BIS_atypical) cases but one (brown) are shown to map with control cases. **(b)** Multidimensional scaling plot shows a clear separation between the BIS-HVDAS discovery and validation cases (red, orange, purple, and pink) used for training and testing and the controls (blue). All BIS_atypical cases but one (brown) are shown to map with control cases. **(c)** Support Vector Machine classifier model. Model was trained using the selected BIS-HVDAS episignature probes, 75% of controls and 75% of other neurodevelopmental disorder samples (blue). The remaining 25% controls and 25% of other disorder samples were used for testing (gray). Plot shows that one of the BIS_atypical cases have methylation variant pathogenicity (MVP) scores close to 1 similar as the training and validation cases. The other BIS_atypical cases show an MVP score close to 0 similar as the control cases. Abbreviations available in Table S3.

HVDAS_validation and BIS_validation and 4 samples with non-NCBRS-non-BIS variants for assessment labeled as BIS_atypical. Hierarchical clustering and MDS confirmed that all validation cases clustered together with the training cases. The SVM classifier model showed that all validation cases had an MVP score close to 1 indicating a common BIS-HVDAS episignature. However, of the 4 BIS_atypical cases, only one (case 31) clustered with the BIS-HVDAS episignature positive cohort (Figure 2).

To further optimize the classifier, we performed an additional round of episignature discovery combining the discovery and the validation positive cases ($n = 23$) in the training cohort. We detected 239 differentially methylated CpG probes (Table S2), which was our final set of selected probes. All cases clustered together in heatmap and MDS and the MVP score was all close to 1 indicating the presences of the BIS-HVDAS episignature (Figure S3). To test the robustness of the final episignature, we again performed 20 rounds of leave-25%-out cross validation, using our unsupervised hierarchical and MDS clustering methods, and all of the cases clustered together with the remaining training cases (Figure S4).

### 3.1.1 | Overlap of the BIS-HVDAS genome-wide DNA methylation profile with other neurodevelopmental disorders on EpiSign™

To further functionally characterize the genome-wide DNA methylation profiles in the BIS-HVDAS patient cohort, we annotated the genomic locations of the DMPs in relation to CpG islands and genes and compared it to 56 other episignature disorders (Figure 3). Quantification of genome-wide methylation changes showed a relatively hypomethylated profile (Figure 4a). Clustering analyses using up to the 500 most significant DMPs for each cohort showed highest percentage of overlap with HVDAS (ADNP syndrome [Central] HVDAS_C, 26%) (Figure S5, Figure 4b).

Finally, we investigated the degree of relatedness between BIS-HVDAS and other episignature cohorts. In the tree and leaf plot, we showed the DMP overlap and the hypermethylation or hypermethylation levels with binary tree where each node represents an episignature cohort; highlighting that BIS-HVDAS cohort clustered in the hypomethylated branch proximal to HVDAS (ADNP syndrome [Central] HVDAS_C) cohort (Figure 5).

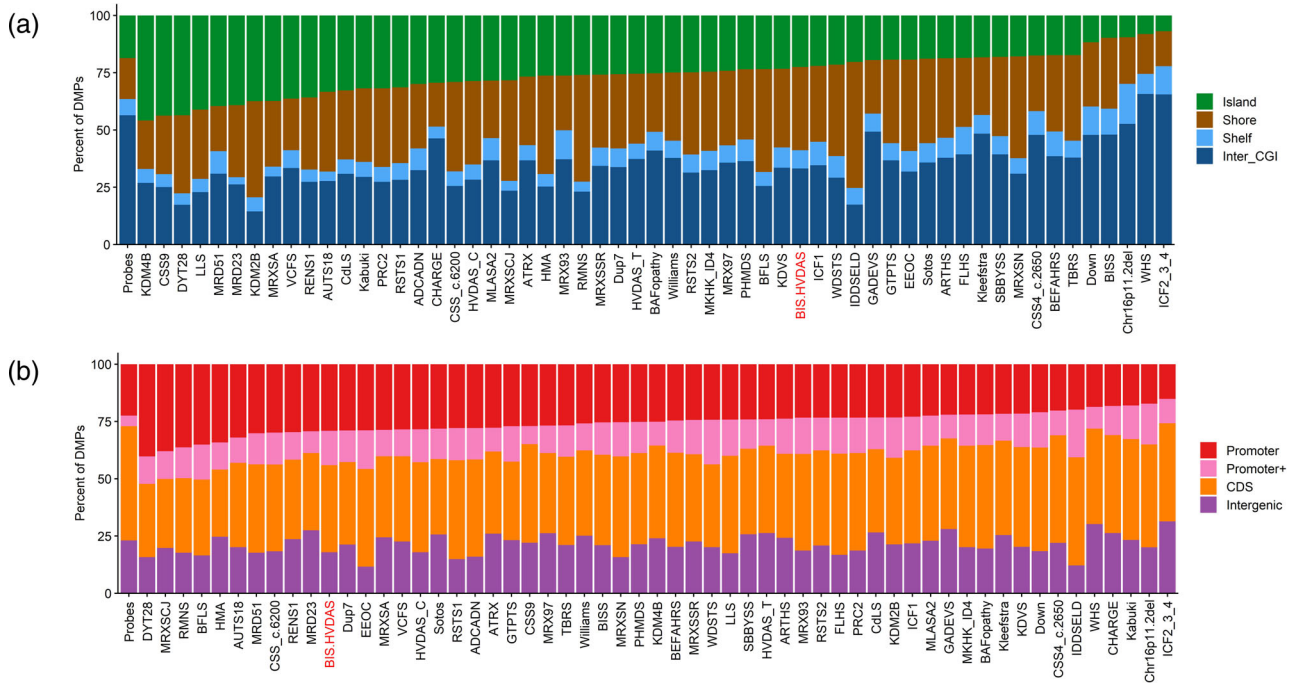


**FIGURE 3** Differentially methylated probes (DMPs) annotated in the context of CpG islands and genes. **(a)** DMPs in relation to genes. **(b)** DMPs in CpG island. Promoter, 0–1 kb upstream of the transcription start site (TSS); Promoter+, 1–5 kb upstream of the TSS; CDS, coding sequence; Intergenic, all other regions of the genome. Island, CpG islands; Shore, within 0–2 kb of a CpG island boundary; shelf, within 2–4 kb of a CpG island boundary; Inter_CGI, all other regions in the genome. The Probes column in both (b,d) represents the background distribution determined in the Levy et al. study of all array probes after initial filtering and used as input for DMP analysis. Abbreviations available in Table S3.

## 4 | DISCUSSION

Episignature analysis is a novel diagnostic modality that can be used to screen patients and reclassify ambiguous genetic findings based on highly sensitive and specific DNA methylation biomarkers detectable in easily accessible peripheral blood specimens (Sadikovic et al., 2021). It enables increased diagnostic yield beyond the current limitations of standard DNA sequencing, including reclassification of coding and non-coding variants of uncertain significance (VUS) (Aref-Eshghi et al., 2020; Sadikovic et al., 2019). Furthermore, DNA methylation episignatures enabled delineation of distinct subtypes in clinically related syndromes with shared pathophysiology including disorders due to *SMARCA2* variants (Cappuccio et al., 2020).

Considering the clinical similarity among patients with pathogenic class II *ADNP* variants and those with *SMARCA2* missense variants leading to the BIS phenotype, we hypothesized a common molecular pathophysiology between HVDAS and BIS. Following an in-depth phenotypic analysis, we verified the clinical convergence between the two syndromes, further substantiated by the shared DNA methylation pattern detectable in the peripheral blood's DNA of the affected individuals. In contrast to *SMARCA2* pathogenic variants resulting in NCBRS or BIS, the two distinct methylation profiles in the *ADNP* gene have previously been associated with only modest differences in behavioral phenotypes (Vandeweyer et al., 2014), but without any in-depth facial dysmorphology delineation. Subjects with *ADNP* class II methylation variants and subjects with *SMARCA2*-BIS showed overlapping epi-signatures, suggesting an epigenotype–phenotype correlation, supported by a common pathogenic mechanism. Most *ADNP* variants located in the nuclear bipartite localization domain (BNL domain), play a critical role in transport to the nucleus: variants in the first basic region of BNL domain, such as the p.(Tyr719*), confine *ADNP* to the cytoplasm, whereas variants in the second region, such as the p. (Arg730*), manage to import into the nucleus the mutant *ADNP* form (Cappuyns et al., 2018; Ganaiem et al., 2022). Despite these two variants result in different ADNP subcellular localization and perhaps functional effects, they both lead to the same methylation profile. Therefore, the mechanisms resulting in the same genome methylation defect remains to be investigated. We speculate that class II *ADNP* variants and BIS-causing *SMARCA2* variants disrupt the chromatin remodeling activity of the BAF complexes, thus explaining their functional overlap. ADNP directly binds genomic DNA and mediates the recruitment of the BAF complex through its C-terminal end. It has been hypothesized that the mutated protein still binds to the DNA, but is no longer capable of recruiting the BAF complex, leading to diminished functionality of the complex and ultimately to deregulation of several genes (Helsmoortel et al., 2014).

*ADNP* has also been shown to interact with the chromatin-remodeling gene *CHD4* (D'Incal et al., 2023) and pathogenic variants in *CHD4* are responsible for a rare condition characterized by intellectual disability, multiple congenital anomalies and dysmorphic facial features including short palpebral fissures (Weiss et al., 2020). Genome methylation studies on these cases have not been yet

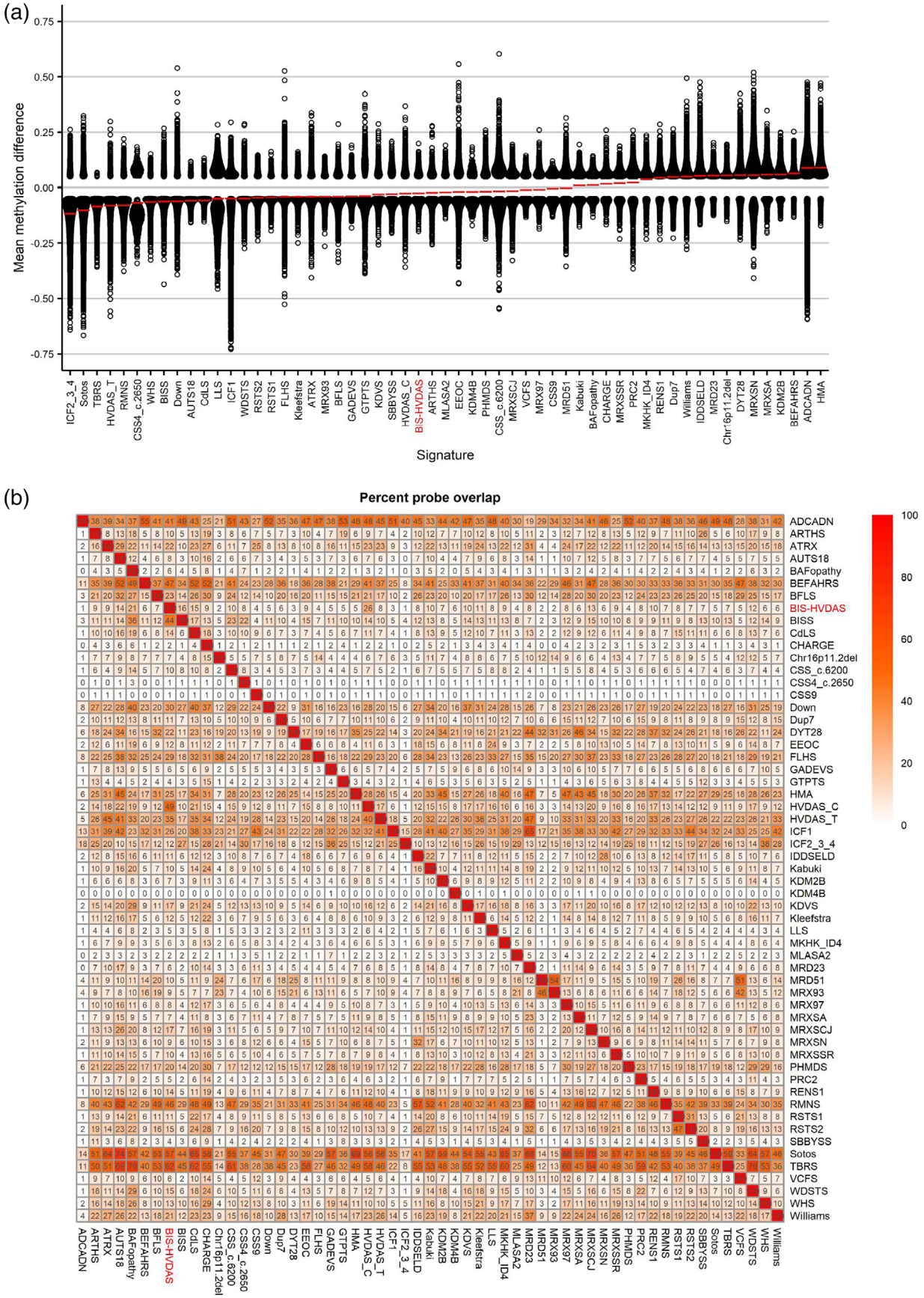


**FIGURE 4** Legend on next page.

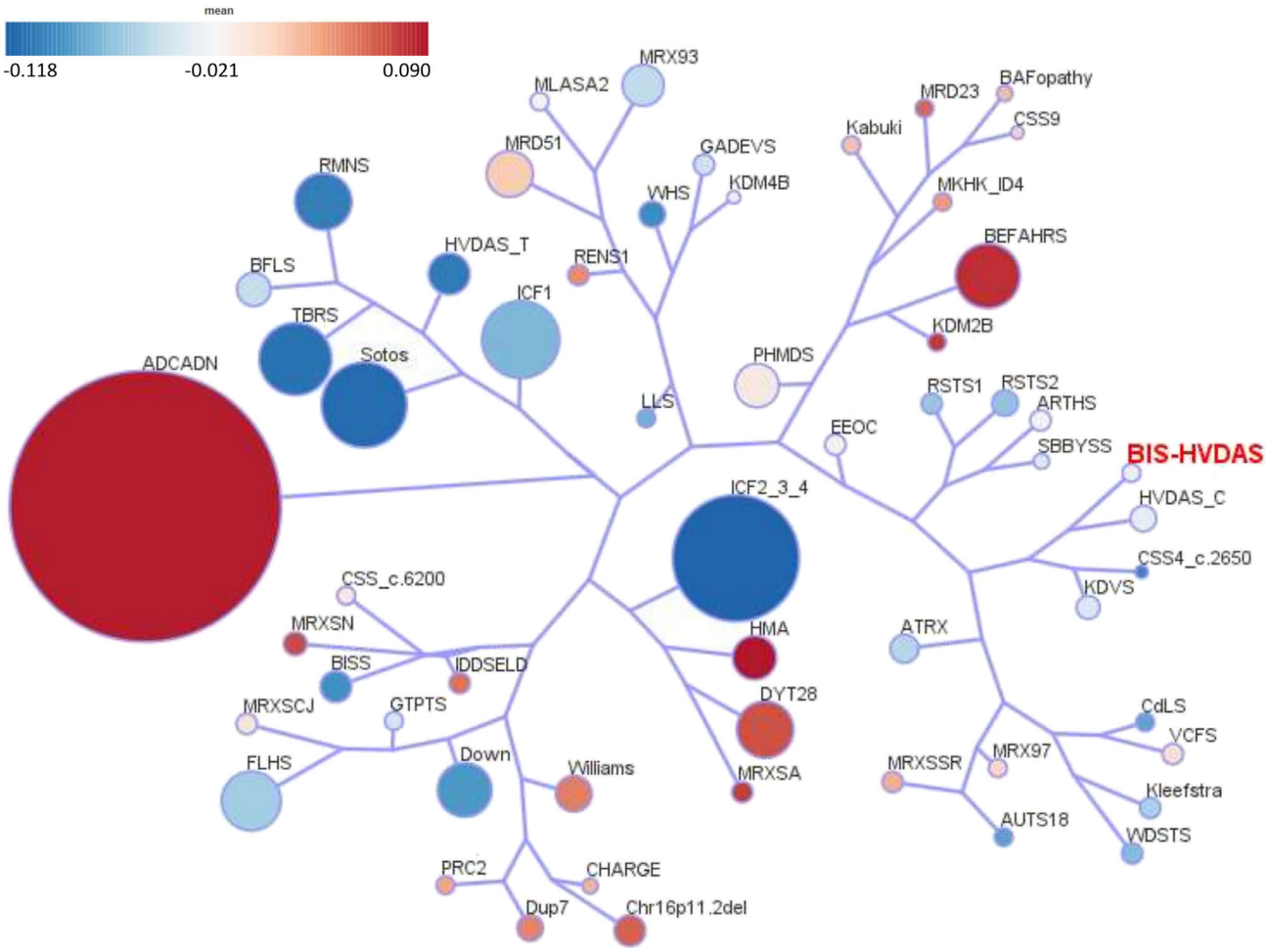


**FIGURE 5** Tree and leaf visualization of Euclidean clustering of all 57 cohorts using the top *n* DMPs for each group, where $n = \min$ (# of DMPs, 500). Cohort samples were aggregated using the median value of each probe within a group. A leaf node represents a cohort, with node sizes illustrating relative scales of the number of selected DMPs for the corresponding cohort, and node colors are indicative of the global mean methylation difference. Abbreviations available in Table S3.

performed, but it is tempting to hypothesize an overlap with HVDAS-class II-ADNP and BIS-SMARCA2 cases.

By binding to chromatin remodelers (BAF and CHD complex), *ADNP* controls chromatin accessibility and nucleosome configuration (Sun et al., 2020). Therefore, ADNP defects could result in disruption of proper chromatin structure that might in turn result in aberrant DNA methylation. In conclusion, our findings confirm that whole genome methylation profile analysis can improve disease identification and classification, allowing more in-depth phenotyping. These findings show evidence of a sensitive phenotype-specific episignature biomarker shared across distinct genetic conditions that also exhibit unique gene-specific episignatures and highlight the utility of episignature biomarkers as diagnostic clinical biomarkers. Evidence of the common episignatures and clinical features in patients with *ADNP* class II variant and *SMARCA2*-BIS provides evidence for common molecular pathophysiology that warrants further investigation.

## AUTHOR CONTRIBUTIONS

*Conceptualization, project administration, and supervision*: BS and NBP. *Data curation*: LVDL, JR, MAL, RR, and JK. *Formal analysis*: LVDL, JR, JK, MAL, and RR. *Investigation*: CS, LVDL, ST, DC, AB, HM, MLT, CK, MA, PH, RCMH, CC, SD, AV, LF, SW, AV-D, LP, AB, TY, KM, MZ, UK, DO, SBS, DW, GC, and NBP. *Validation and visualization*: CS, LVDL,

**FIGURE 4** Relationships between the Blepharophimosis-impaired intellectual development syndrome and Helsmoortel-van der Aa syndrome cohort and 56 other EpiSign™ disorders. **(a)** Global methylation profiles of all differentially methylated probes (DMPs, FDR <0.05) for each cohort, sorted by mean methylation. Each circle represents one probe, red lines show the mean methylation. **(b)** Heatmap showing the percentage of probes shared between each paired cohort. Colors indicate the percentage of the y-axis cohort's probes that are also found in the x-axis cohort's probes. Abbreviations available in Table S3.

and JR. *Writing-original draft*: CS and LVDL. *Writing-review and editing*: CS, LVDL, BS, and NBP.

## ACKNOWLEDGMENTS

We would like to thank the participants and their families described in this study for their participation. This study was supported by Telethon Foundation, Telethon Undiagnosed Diseases Program (TUDP, GSP15001). This study was in part generated within the European Reference Network ITHACA.

## FUNDING INFORMATION

Funding for this study is provided in part by the Government of Canada through Genome Canada and the Ontario Genomics Institute (OGI-188). Liselot van der Laan was awarded with the AR&D Travel grant from the Amsterdam UMC, which provided financial support for this work.

## CONFLICT OF INTEREST STATEMENT

Bekim Sadikovic is a shareholder in EpiSign Inc., a biotech firm involved in commercial application of EpiSign™ technology.

## DATA AVAILABILITY STATEMENT

Some of the datasets used in this study are publicly available and may be obtained from gene expression omnibus (GEO) using the following accession numbers. GEO: GSE116992, GSE66552, GSE74432, GSE97362, GSE116300, GSE95040, GSE 104451, GSE125367, GSE55491, GSE108423, GSE116300, GSE 89353, GSE52588, GSE42861, GSE85210, GSE87571, GSE87648, GSE99863, and GSE35069. These include DNA methylation data from individuals with Kabuki syndrome, Sotos syndrome, CHARGE syndrome, immunodeficiency-centromeric instability-facial anomalies (ICF) syndrome, Williams-Beuren syndrome, Chr7q11.23 duplication syndrome, BAFopathies, down syndrome, a large cohort of unresolved subjects with developmental delays and congenital abnormalities, and also several large cohorts of DNA methylation data from the general population. Remaining data are not available due to institutional or REB restrictions. EpiSign™ is proprietary, trademarked analytical software owned by EpiSign Inc. parts of it are based on the methods and publicly available software that are referenced in the methods section. Detailed description of publicly available software components (R-packages) and parameters used are described previously (Aref-Eshghi et al., 2020; Levy, McConkey, et al., 2022).

## ORCID

*Camilla Sarli* https://orcid.org/0000-0002-5274-8112
*Liselot van der Laan* https://orcid.org/0000-0002-7800-8665
*Jack Reilly* https://orcid.org/0000-0001-7150-9566
*Slavica Trajkova* https://orcid.org/0000-0002-0178-5327
*Diana Carli* https://orcid.org/0000-0001-5690-6504
*Alfredo Brusco* https://orcid.org/0000-0002-8318-7231
*Raissa Relator* https://orcid.org/0000-0002-8153-2222
*Jennifer Kerkhof* https://orcid.org/0000-0003-1245-6606
*Matthew L. Tedder* https://orcid.org/0000-0003-0613-6702
*Cindy Skinner* https://orcid.org/0000-0002-7841-8277
*Mariëlle Alders* https://orcid.org/0000-0002-7386-4868
*Peter Henneman* https://orcid.org/0000-0003-2179-7808
*Claudia Ciaccio* https://orcid.org/0000-0002-4100-7028
*Stefano D'Arrigo* https://orcid.org/0000-0001-5188-9418
*Antonio Vitobello* https://orcid.org/0000-0003-3717-8374
*Laurence Faivre* https://orcid.org/0000-0001-9770-444X
*Sacha Weber* https://orcid.org/0000-0001-9363-5141
*Toshiyuki Yamamoto* https://orcid.org/0000-0002-7540-5040
*Gerarda Cappuccio* https://orcid.org/0000-0003-3934-2342
*Nicola Brunetti-Pierri* https://orcid.org/0000-0002-6895-8819

## REFERENCES

Aref-Eshghi, E., Bend, E. G., Colaiacovo, S., Caudle, M., Chakrabarti, R., Napier, M., Brick, L., Brady, L., Carere, D. A., Levy, M. A., Kerkhof, J., Stuart, A., Saleh, M., Beaudet, A. L., Li, C., Kozenko, M., Karp, N., Prasad, C., Siu, V. M., … Sadikovic, B. (2019). Diagnostic utility of genome-wide DNA methylation testing in genetically unsolved individuals with suspected hereditary conditions. *American Journal of Human Genetics*, *104*(4), 685–700.

Aref-Eshghi, E., Kerkhof, J., Pedro, V. P., Barat-Houari, M., Ruiz-Pallares, N., Andrau, J. C., Lacombe, D., Van-Gils, J., Fergelot, P., Dubourg, C., & Cormier-Daire, V. (2020). Evaluation of DNA methylation episignatures for diagnosis and phenotype correlations in 42 Mendelian neurodevelopmental disorders. *American Journal of Human Genetics*, *106*(3), 356–370.

Aryee, M. J., Jaffe, A. E., Corrada-Bravo, H., Ladd-Acosta, C., Feinberg, A. P., Hansen, K. D., & Irizarry, R. A. (2014). Minfi: A flexible and comprehensive Bioconductor package for the analysis of Infinium DNA methylation microarrays. *Bioinformatics*, *30*(10), 1363–1369.

Bend, E. G., Aref-Eshghi, E., Everman, D. B., Rogers, R. C., Cathey, S. S., Prijoles, E. J., Lyons, M. J., Davis, H., Clarkson, K., Gripp, K. W., Li, D., Bhoj, E., Zackai, E., Mark, P., Hakonarson, H., Demmer, L. A., Levy, M. A., Kerkhof, J., Stuart, A., … Sadikovic, B. (2019). Gene domain-specific DNA methylation episignatures highlight distinct molecular entities of ADNP syndrome. *Clinical Epigenetics*, *11*(1), 64.

Breen, M. S., Garg, P., Tang, L., Mendonca, D., Levy, T., Barbosa, M., Arnett, A. B., Kurtz-Nelson, E., Agolini, E., Battaglia, A., Chiocchetti, A. G., Freitag, C. M., Garcia-Alcon, A., Grammatico, P., Hertz-Picciotto, I., Ludena-Rodriguez, Y., Moreno, C., Novelli, A., Parellada, M., … de Rubeis, S. (2020). Episignatures stratifying Helsmoortel-Van Der aa syndrome show modest correlation with phenotype. *American Journal of Human Genetics*, *107*(3), 555–563.

Cappuccio, G., Sayou, C., Tanno, P. L., Tisserant, E., Bruel, A. L., Kennani, S. E., Sá, J., Low, K. J., Dias, C., Havlovicová, M., Hančárová, M., Eichler, E. E., Devillard, F., Moutton, S., van Gils, J., Dubourg, C., Odent, S., Gerard, B., Piton, A., … Brunetti-Pierri, N. (2020). De novo SMARCA2 variants clustered outside the helicase domain cause a new recognizable syndrome with intellectual disability and blepharophimosis distinct from Nicolaides-Baraitser syndrome. *Genetics in Medicine*, *22*(11), 1838–1850.

Cappuyns, E., Huyghebaert, J., Vandeweyer, G., & Kooy, R. F. (2018). Mutations in ADNP affect expression and subcellular localization of the protein. *Cell Cycle*, *17*(9), 1068–1075.

Cardoso, M. A., Rizzardi, L. E. A., Kume, L. W., Groeneveld, C. S., Trefflich, S., Morais, D. A. A., Dalmolin, R. J. S., Ponder, B. A. J., Meyer, K. B., & Castro, M. A. A. (2022). TreeAndLeaf: An R/-Bioconductor package for graphs and trees with focus on the leaves. *Bioinformatics*, *38*(5), 1463–1464.

Cavalcante, R. G., & Sartor, M. A. (2017). Annotatr: Genomic regions in context. *Bioinformatics*, *33*(15), 2381–2383.

D'Incal, C. P., Van Rossem, K. E., De Man, K., Konings, A., Van Dijck, A., Rizzuti, L., Vitriolo, A., Testa, G., Gozes, I., Vanden Berghe, W., & Kooy, R. F. (2023). Chromatin remodeler activity-dependent neuroprotective protein (ADNP) contributes to syndromic autism. *Clinical Epigenetics*, *15*(1), 45.

Ganaiem, M., Karmon, G., Ivashko-Pachima, Y., & Gozes, I. (2022). Distinct impairments characterizing different ADNP mutants reveal aberrant cytoplasmic-nuclear crosstalk. *Cells*, *11*(19), 2994.

Gu, Z., Gu, L., Eils, R., Schlesner, M., & Brors, B. (2014). Circlize implements and enhances circular visualization in R. *Bioinformatics*, *30*(19), 2811–2812.

Helsmoortel, C., Vulto-van Silfhout, A. T., Coe, B. P., Vandeweyer, G., Rooms, L., van den Ende, J., Schuurs-Hoeijmakers, J. H., Marcelis, C. L., Willemsen, M. H., Vissers, L. E., & Yntema, H. G. (2014). A SWI/SNF-related autism syndrome caused by de novo mutations in ADNP. *Nature Genetics*, *46*(4), 380–384.

Ho, D., Imai, K., King, G., & Stuart, E. A. (2011). MatchIt: Nonparametric preprocessing for parametric causal inference. *Journal of Statistical Software.*, *42*(8), 1–28.

Krajewska-Walasek, M., Jurkiewicz, D., Piekutowska-Abramczuk, D., Kucharczyk, M., Chrzanowska, K. H., Jezela-Stanek, A., & Ciara, E. (2016). Additional data on the clinical phenotype ofHelsmoortel-Van der Aa syndrome associated with a novel truncating mutation inADNP gene. *American Journal of Medical Genetics. Part A*. *170*(6), 1647–1650.

Levy, M. A., McConkey, H., Kerkhof, J., Barat-Houari, M., Bargiacchi, S., Biamino, E., Bralo, M. P., Cappuccio, G., Ciolfi, A., Clarke, A., DuPont, B., Elting, M. W., Faivre, L., Fee, T., Fletcher, R. S., Cherik, F., Foroutan, A., Friez, M. J., Gervasini, C., … Sadikovic, B. (2022). Novel diagnostic DNA methylation episignatures expand and refine the epigenetic landscapes of Mendelian disorders. *HGG Adv*, *3*(1), 100075.

Levy, M. A., Relator, R., McConkey, H., Pranckeviciene, E., Kerkhof, J., Barat-Houari, M., Bargiacchi, S., Biamino, E., Palomares Bralo, M., Cappuccio, G., Ciolfi, A., Clarke, A., DuPont, B. R., Elting, M. W., Faivre, L., Fee, T., Ferilli, M., Fletcher, R. S., Cherick, F., … Sadikovic, B. (2022). Functional correlation of genome-wide DNA methylation profiles in genetic neurodevelopmental disorders. *Human Mutation*, *43*, 1609–1628.

Oz, S., Ivashko-Pachima, Y., & Gozes, I. (2012). The ADNP derived peptide, NAP modulates the tubulin pool: Implication for neurotrophic and neuroprotective activities. *PLoS ONE*, *7*(12), e51458.

Pascolini, G., Agolini, E., Majore, S., Novelli, A., Grammatico, P., & Digilio, M. C. (2018). Helsmoortel-Van der Aa Syndrome as emerging clinical diagnosis in intellectually disabled children with autistic traits and ocular involvement. *Eur J Paediatr Neurol*. *22*(3), 552–557.

Richards, S., Aziz, N., Bale, S., Bick, D., Das, S., Gastier-Foster, J., Grody, W. W., Hegde, M., Lyon, E., Spector, E., & Voelkerding, K. (2015). Standards and guidelines for the interpretation of sequence variants: A joint consensus recommendation of the American College of Medical Genetics and Genomics and the Association for Molecular Pathology. *Genetics in Medicine*, *17*(5), 405–424.

Riggs, E. R., Andersen, E. F., Cherry, A. M., Kantarci, S., Kearney, H., Patel, A., Raca, G., Ritter, D. I., South, S. T., Thorland, E. C., Pineda-Alvarez, D., Aradhya, S., & Martin, C. L. (2020). Technical standards for the interpretation and reporting of constitutional copy-number variants: A joint consensus recommendation of the American College of Medical Genetics and Genomics (ACMG) and the clinical genome resource (ClinGen). *Genetics in Medicine*, *22*(2), 245–257.

Ritchie, M. E., Phipson, B., Wu, D., Hu, Y., Law, C. W., Shi, W., & Smyth, G. K. (2015). Limma powers differential expression analyses for RNA-sequencing and microarray studies. *Nucleic Acids Research*, *43*(7), e47.

Rooney, K., van der Laan, L., Trajkova, S., Haghshenas, S., Relator, R., Lauffer, P., Vos, N., Levy, M. A., Brunetti-Pierri, N., Terrone, G., Mignot, C., Keren, B., de Villemeur, T. B., Volker-Touw, C. M. L., Verbeek, N., van der Smagt, J. J., Oegema, R., Brusco, A., Ferrero, G. B., … Henneman, P. (2023). DNA methylation episignature and comparative epigenomic profiling of HNRNPU-related neurodevelopmental disorder. *Genetics in Medicine*, *25*(8), 100871.

Sadikovic, B., Aref-Eshghi, E., Levy, M. A., & Rodenhiser, D. (2019). DNA methylation signatures in mendelian developmental disorders as a diagnostic bridge between genotype and phenotype. *Epigenomics*, *11*(5), 563–575.

Sadikovic, B., Levy, M. A., Kerkhof, J., Aref-Eshghi, E., Schenkel, L., Stuart, A., McConkey, H., Henneman, P., Venema, A., Schwartz, C. E., Stevenson, R. E., Skinner, S. A., DuPont, B. R., Fletcher, R. S., Balci, T. B., Siu, V. M., Granadillo, J. L., Masters, J., Kadour, M., … Alders, M. (2021). Clinical epigenomics: Genome-wide DNA methylation analysis for the diagnosis of Mendelian disorders. *Genetics in Medicine*, *23*(6), 1065–1074.

Sun, X., Yu, W., Li, L., & Sun, Y. (2020). ADNP controls gene expression through local chromatin architecture by association with BRG1 and CHD4. *Frontiers in Cell and Development Biology*, *8*, 553.

Takenouchi, T., Miwa, T., Sakamoto, Y., Sakaguchi, Y., Uehara, T., Takahashi, T., & Kosaki, K. (2017). Further evidence that ablepharophimosis syndrome phenotype is associated with a specific class ofmutation in the ADNP gene. *American Journal of Medical Genetics Part A*, *173*(6), 1631–1634.

van der Laan, L., Rooney, K., Alders, M., Relator, R., McConkey, H., Kerkhof, J., Levy, M. A., Lauffer, P., Aerden, M., Theunis, M., Legius, E., Tedder, M. L., Vissers, L. E. L. M., Koene, S., Ruivenkamp, C., Hoffer, M. J. V., Wieczorek, D., Bramswig, N. C., Herget, T., … Henneman, P. (2022). Episignature mapping of TRIP12 provides functional insight into Clark–Baraitser syndrome. *International Journal of Molecular Sciences.*, *23*(22), 13664.

Van Dijck, A., Vulto-van Silfhout, A. T., Cappuyns, E., van der Werf, I. M., Mancini, G. M., Tzschach, A., Bernier, R., Gozes, I., Eichler, E. E., Romano, C., & Lindstrand, A. (2019). Clinical presentation of a complex neurodevelopmental disorder caused by mutations in ADNP. *Biological Psychiatry*, *85*(4), 287–297.

Vandeweyer, G., Helsmoortel, C., Van Dijck, A., Vulto-van Silfhout, A. T., Coe, B. P., Bernier, R., Gerdts, J., Rooms, L., Van Den Ende, J., Bakshi, M., & Wilson, M. (2014). The transcriptional regulator ADNP links the BAF (SWI/SNF) complexes with autism. *American Journal of Medical Genetics. Part C, Seminars in Medical Genetics*, *166c*(3), 315–326.

Weiss, K., Lazar, H. P., Kurolap, A., Martinez, A. F., Paperna, T., Cohen, L., Smeland, M. F., Whalen, S., Heide, S., Keren, B., Terhal, P., Irving, M., Takaku, M., Roberts, J. D., Petrovich, R. M., Schrier Vergano, S. A., Kenney, A., Hove, H., DeChene, E., … Lachlan, K. (2020). The CHD4-related syndrome: A comprehensive investigation of the clinical spectrum, genotype-phenotype correlations, and molecular basis. *Genetics in Medicine*, *22*(2), 389–397.

## SUPPORTING INFORMATION

Additional supporting information can be found online in the Supporting Information section at the end of this article.

**How to cite this article:** Sarli, C., van der Laan, L., Reilly, J., Trajkova, S., Carli, D., Brusco, A., Levy, M. A., Relator, R., Kerkhof, J., McConkey, H., Tedder, M. L., Skinner, C., Alders, M., Henneman, P., Hennekam, R. C. M., Ciaccio, C., D'Arrigo, S., Vitobello, A., Faivre, L., … Brunetti-Pierri, N. (2024). Blepharophimosis with intellectual disability and Helsmoortel-Van Der Aa Syndrome share episignature and phenotype. *American Journal of Medical Genetics Part C: Seminars in Medical Genetics*, e32089. https://doi.org/10.1002/ajmg.c.32089